Electronic Supplementary Material (ESI) for Polymer Chemistry.
This journal is © The Royal Society of Chemistry 2023

Supporting information

A single monomer difference can impact the nanostructure output of precision oligo(phosphodiesters)

Donatien de Rochambeau,[a] Maciej Barłóg,[b] Felix J. Rizzuto,[c] Quentin Laurent,[a] Xin Luo,[a] Kai Lin Lau,[a] Hassan S. Bazzi[b] and Hanadi F. Sleiman*[a]

a. Department of Chemistry, McGill University, 801, Sherbrooke St. West, Montreal, QC, Canada. H3A 0B8; b. Division of Art and Science, Texas A&M University at Qatar, P.O. Box 23874, Doha, Qatar; c. School of Chemistry, University of New South Wales, Sydney, Australia 2052.

*E-mail: hanadi.sleiman@mcgill.ca

Contents

1. Chemicals

All starting materials were obtained from commercial suppliers and used without further purification unless otherwise noted. Acetic acid, boric acid, solvents were purchased from Fisher Scientific. Choroform-d_3 was purchased from Cambridge Isotope Laboratories. Importantly, it was stored on molecular sieves in order to keep it neutral. If used as sold, hydrolysis of phosphoramidite (fast) as well as DMT deprotection (slow) may be observed. GelRed™ nucleic acid stain was purchased from Biotium Inc. Concentrated ammonium hydroxide, ammonium persulfate, acrylamide/Bis-acrylamide (40% 19:1 solution) and TEMED were obtained from Bioshop Canada Inc. and used as supplied. 1 μmol Universal 1000Å LCAA-CPG supports and standard reagents used for automated DNA and RNA synthesis were purchased through Bioautomation. N,N-diisopropylamino Cyanoethyl phosphonamidic-chloride (CEP-Cl) and DMT-hexaethyloxy glycol (cat.# CLP-9765) phosphoramidites were purchased from Chemgenes. Sephadex G-25 (super fine, DNA grade) was purchased from Glen Research. All other reagents were obtained from Sigma-Aldrich. TEAA buffer is composed of 50mM TEA with pH adjusted to 8.0 using glacial acetic acid. TBE buffer is 90 mM Tris, 90 mM boric acid and 1.1 mM EDTA with a pH of 8.0. TAMg buffer is 40 mM Tris, 7.6 mM magnesium chloride and 1.4 mM acetic acid. TA5Mg buffer is similar than TAMg but with 38 mM magnesium chloride. Muscovite Ruby mica sheets (grade 2) were used as substrate for all AFM imaging studies.

Abbreviations. ACN: Acetonitrile; AFM: Atomic force microscopy; AGE: Agarose gel electrophoresis; CPG: Controlled pore glass; DIPEA: Diisopropylethylamine; DLS: Dynamic light scattering; DMT: Dimethoxytrytil; ESI: Electrospray ionization; ETT: 5-(ethylthio)-1H-tetrazole; HOPG: Highly-ordered pyrolytic graphite; HPLC: High-pressure liquid chromatography; LC: Liquid chromatography; LCAA: Long chain alkylamine; MS: Mass spectrometry; PAGE: Polyacrylamide gel electrophoresis; QTOF: Quadrupole time-of-flight; RP: Reverse phase; TEA: Triethylamine; TEAA: Triethylammonium acetate; TEM: Transmission electron microscopy; TEMED: Tetramethylethylenediamine; TLC: Thin layer chromatography; Tris: Trisaminomethane;

2. Instrumentation.

Standard automated solid-phase synthesis was performed on a Mermade MM6 synthesizer from Bioautomation. HPLC purification was carried out on an Agilent Infinity 1260. DNA and oligomers quantification measurements were performed by UV absorbance with a NanoDrop Lite spectrophotometer from Thermo Scientific. For structure assembly, Eppendorf Mastercycler 96-well thermocycler and Bio-Rad T100TM thermal cycler were used to anneal all oligomers. Polyacrylamide gel electrophoresis (PAGE) experiments were carried out on a 20 X 20 cm vertical Hoefer 600 electrophoresis unit while agarose gel electrophoresis (AGE) experiments were performed with an Owl Mini gel electrophoresis unit. Gel images were captured using a ChemiDoc™ MP System from Bio-Rad Laboratories. Gel images were captured using a ChemiDoc™ MP System from Bio-Rad Laboratories. Dry solvents were taken from an Innovation Technology device. LC-ESI-MS of oligomers was carried out using Dionex Ultimate 3000 coupled to a Bruker MaXis Impact™ QTOF. DLS experiments were carried out using a DynaPro™ Instrument from Wyatt Technology. AFM was performed with a MultiModeTM MM8 SPM connected to a NanoscopeTM controller, from the Digital Instruments Veeco Metrology Group. TEM was performed with a LVEM5 from Delong America.

3. Synthesis of Phosphoramidites

The phosphoramidites used to perform solid-phase synthesis were synthesized according to literature procedures.

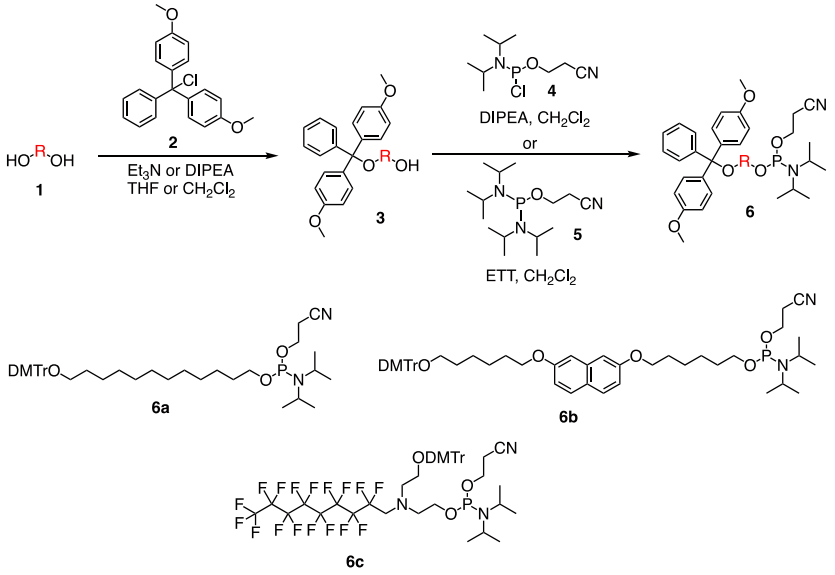

Scheme S1. Synthesis of phosphoramidites following reported procedures for **6a**,[1] **6b**[1] and **6c**.[2]

4. Solid-Phase Synthesis

Standard oligomer synthesis was performed on a 1 μmol scale, starting from a universal 1000 Å LCAA-CPG solid support. Amidite **HEG** was dissolved in dry acetonitrile and all other amidites were dissolved in dry CH_2Cl_2 to obtain 0.1 M solutions. Extended coupling times of 10 minutes were used. Other reagents (oxidizing solution, capping solutions, activator solution) are the same than for standard DNA synthesis. Removal of the DMT protecting group was carried out using 3% dichloroacetic acid in CH_2Cl_2 on the DNA synthesizer.

Completed syntheses were cleaved from the solid support and deprotected in a 1:1 mixture 28% aqueous ammonium hydroxide solution/methylamine 40 wt.% in H_2O for 3 h at 60 °C. The crude product solution was separated from the solid support and concentrated under reduced pressure at 60 °C. This crude solid was re-suspended in 1 mL Millipore water. Filtration with 0.22 μm centrifugal filter was then performed prior to HPLC purification. The resulting solution was quantified by absorbance at 260 nm.

For HPLC purification, solvents were (0.22 μm filtered): 50 mM TEAA buffer (pH 8.0) and HPLC grade acetonitrile. Column: Hamilton PRP-C_{18} 5 μm 100 Å 2.1 x 150 mm was used at 60 °C. For each analytical separation approximately 0.5 OD_{260} of crude oligomer was injected as a 20-50 μL solution in Millipore water. Detection was carried out using a diode-array detector, monitoring absorbance at 260 nm.

To quantify the oligomers in solution, absorbance at 260 nm was measured using a Nanodrop Lite spectrophotometer. Extinction coefficients were calculated according to the following formula:

$\varepsilon = \varepsilon_{\mathbf{NAP}}$ x number of **NAP** in the sequence with $\varepsilon_{\mathbf{NAP}} = 2.80\ mM^{-1}.cm^{-1}$ as reported elsewhere.[1]

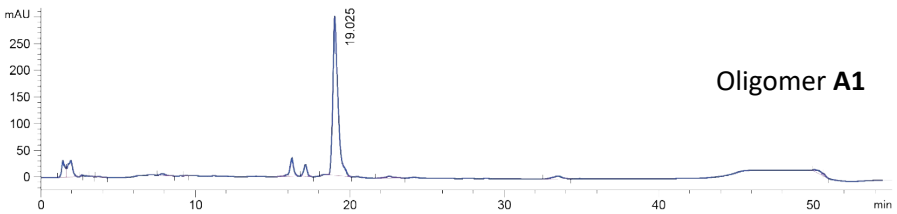

Oligomer **A1**

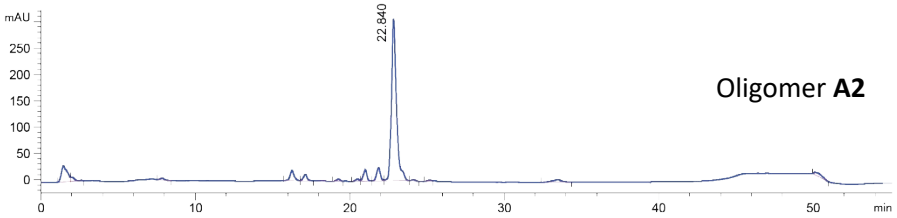

Oligomer **A2**

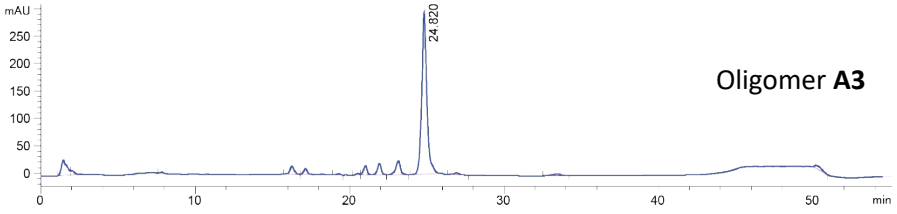

Oligomer **A3**

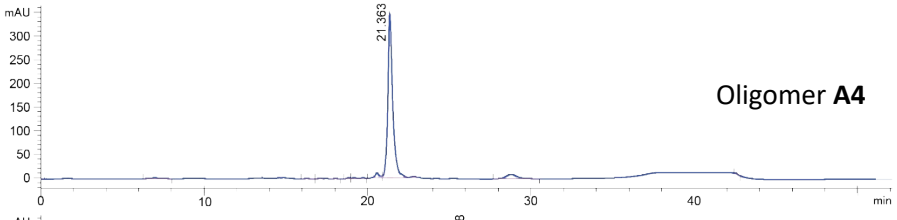

Oligomer **A4**

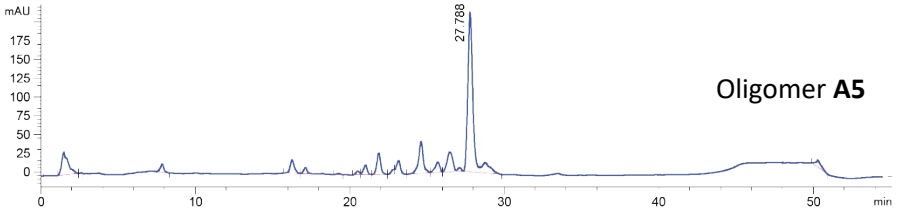

Oligomer **A5**

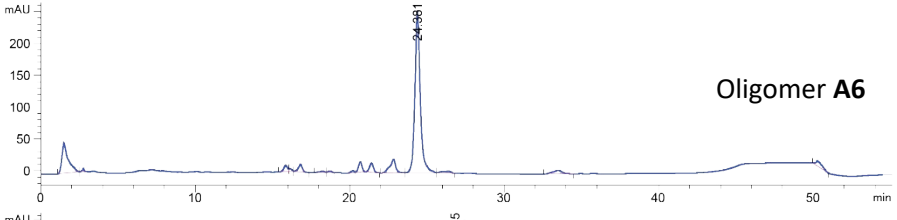

Oligomer **A6**

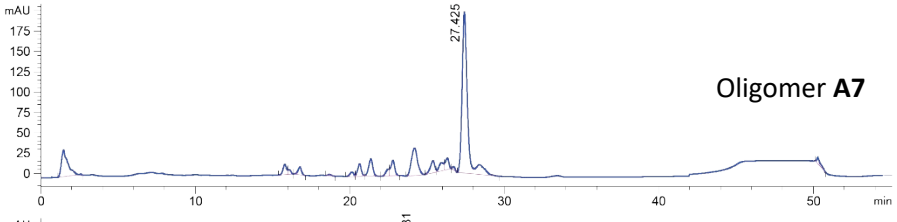

Oligomer **A7**

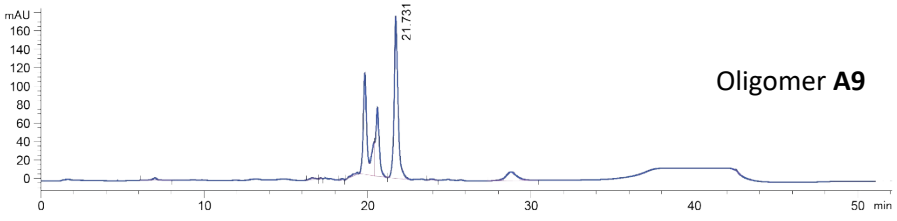

Oligomer **A9**

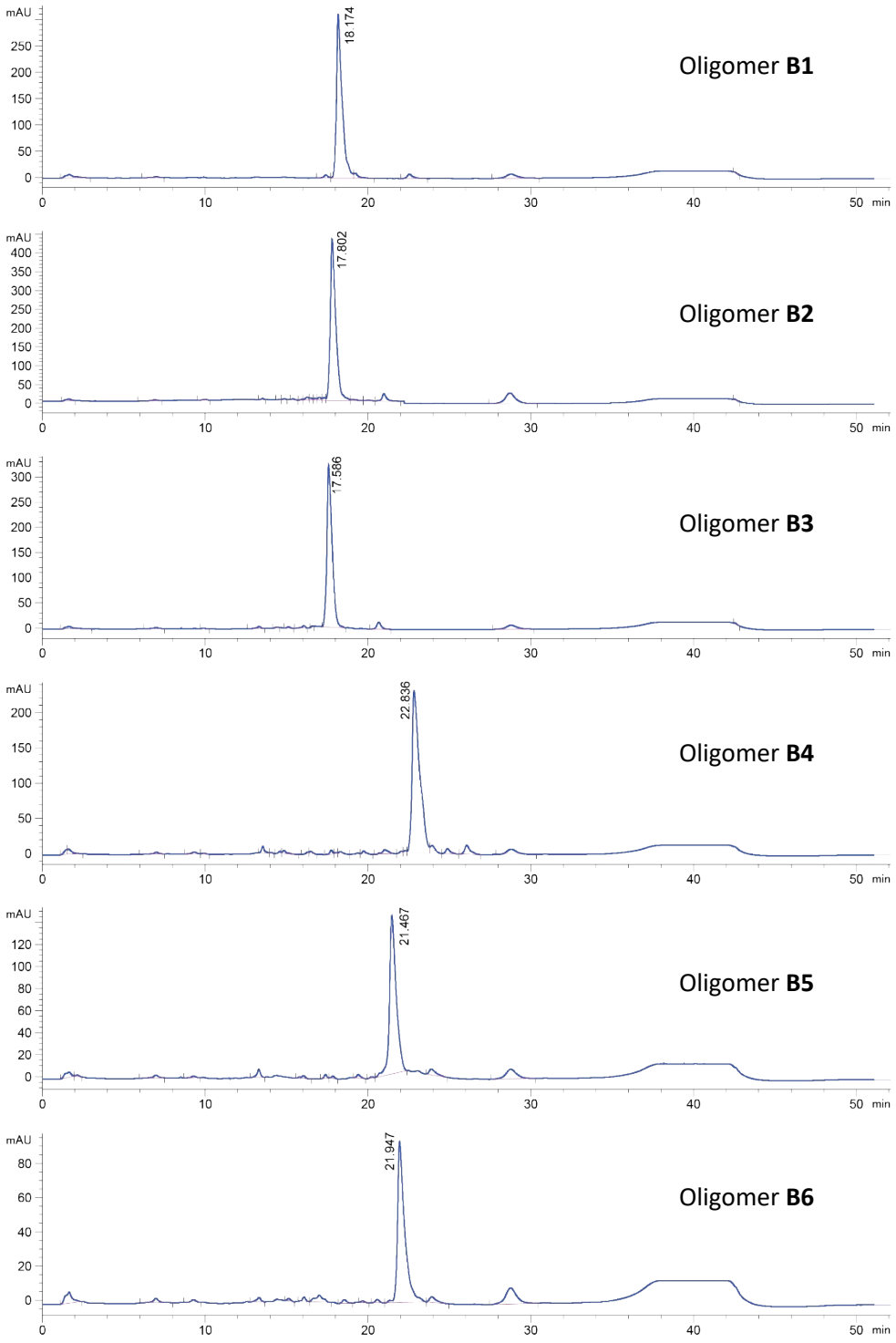

Figure S1. Reverse-phase HPLC traces of crude mixtures for oligomers **A1** – **A7** and **B1** – **B6** (UV detection, 260 nm, gradient 3 – 80% ACN over 30 min for **A4**, over 40 min for all other oligomers).

5. Gel Electrophoresis Purification

For **NAP**$_8$-**HEG**$_{12}$, purification could not be carried out using RP-HPLC, **HEG** being the last monomer added. In that case as well as in the cases of **HEG**$_6$-**NAP**$_3$ and **HEG**$_6$-**NAP**$_6$, crude products were purified on 20% polyacrylamide gels, supplemented with 8 M urea (loading of 0.5 to 2 OD of crude oligomer per gel). Electrophoresis was run at lower voltage (250 V) for the first 30 min followed by 1 h at 500 V. Following electrophoresis, the gel was wrapped in plastic and visualized by UV shadowing over a fluorescent TLC plate. The main band was quickly excised, and the "crush and soak" procedure was applied. It was crushed, and incubated in ~10 mL of autoclaved water, chilled in liquid N_2 for a few minutes and left at 65 °C overnight. The supernatant was then concentrated to 1.0 mL and desalted through size exclusion chromatography (Glen Gel-Pak™ 2.5 Desalting Column from GlenResearch).

6. LC-ESI-MS Characterization

The oligomers were analyzed by LC-ESI-MS in negative ESI mode. Samples (10 to 25 μM, 12 μL) were run through an Acclaim RSLC 120 C_{18} column (2.2 μm, 120 Å 2.1 x 50 mm) using a gradient of mobile phase A (100 mM 1,1,1,3,3,3-hexafluoro-2-propanol and 5 mM TEA in water) and mobile phase B (Methanol) in 8 minutes (2% to 100% B).

Table S1. ESI-MS characterization of the oligomers.

Oligomer	Sequence	Calculated exact mass [g mol^{-1}]	Found exact mass[a] [g mol^{-1}]
A1	**HEG$_4$-NAP**	1736.72	1736.73
A2	**HEG$_4$-NAP$_2$**	2158.91	2158.93
A3	**HEG$_4$-NAP$_3$**	2581.10	2581.11
A4	**HEG$_4$-NAP$_4$**	3003.28	3003.04
A5	**HEG$_4$-NAP$_6$**	3847.67	3847.67
A6	**HEG$_6$-NAP$_3$**	3269.35	3269.36
A7	**HEG$_6$-NAP$_6$**	4535.92	4535.94
A8	**NAP$_8$-HEG$_{12}$**	7445.01	7445.12
A9	**NAP$_2$-HEG$_4$-NAP$_2$**	3003.28	3003.24
B1	**HEG$_4$-C12$_4$-NAP**	2793.32	2793.27
B2	**HEG$_4$-NAP-C12$_4$**	2793.32	2793.34
B3	**HEG$_6$-NAP-C12$_4$**	3481.57	3481.51
B4	**HEG$_4$-NAP-PFC$_4$**	4132.79	4132.52
B5	**HEG$_6$-NAP-PFC$_4$-C12$_4$**	5877.63	5877.72
B6	**HEG$_6$-NAP-C12$_4$-PFC$_4$**	5877.63	5877.73

a. Mass was found using ESI-MS technique, detecting multiply charged species except for oligomers **A1**-**A2** (Figure S3)

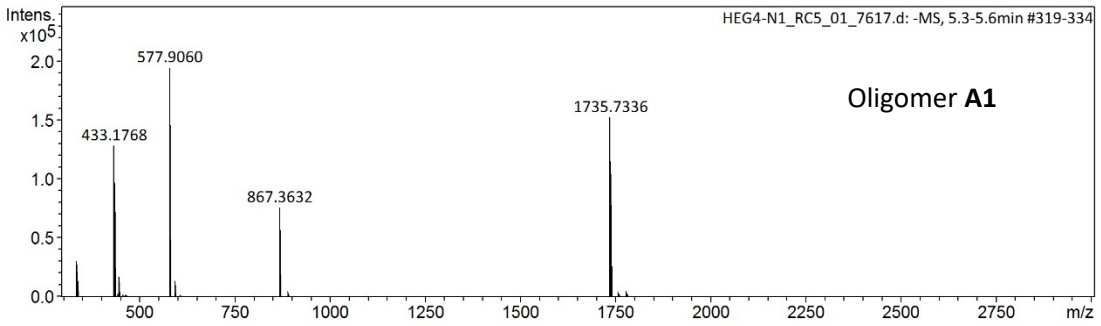
HEG4-N1_RC5_01_7617.d: -MS, 5.3-5.6min #319-334
Intens.
x10^5
577.9060
433.1768
867.3632
1735.7336
Oligomer **A1**
m/z

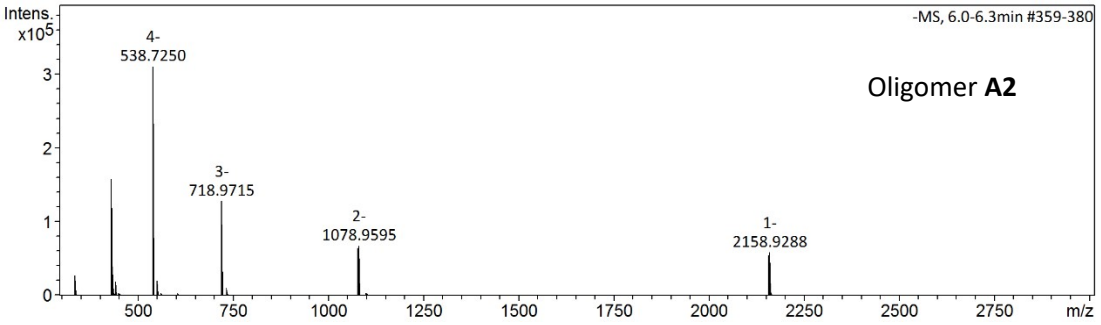
-MS, 6.0-6.3min #359-380
Intens.
x10^5
4-
538.7250
3-
718.9715
2-
1078.9595
1-
2158.9288
Oligomer **A2**
m/z

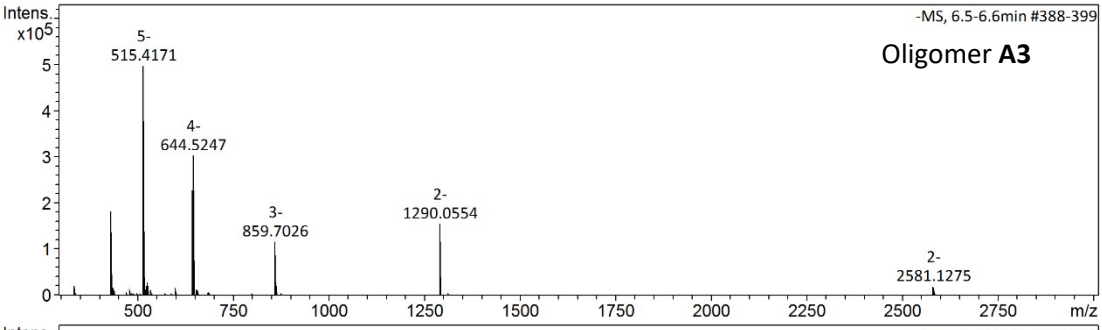
-MS, 6.5-6.6min #388-399
Intens.
x10^5
5-
515.4171
4-
644.5247
3-
859.7026
2-
1290.0554
2-
2581.1275
Oligomer **A3**
m/z

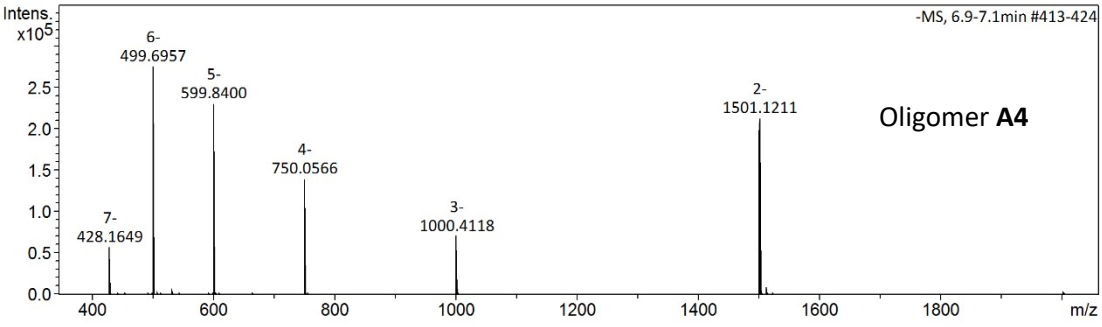
-MS, 6.9-7.1min #413-424
Intens.
x10^5
6-
499.6957
5-
599.8400
4-
750.0566
3-
1000.4118
2-
1501.1211
7-
428.1649
Oligomer **A4**
m/z

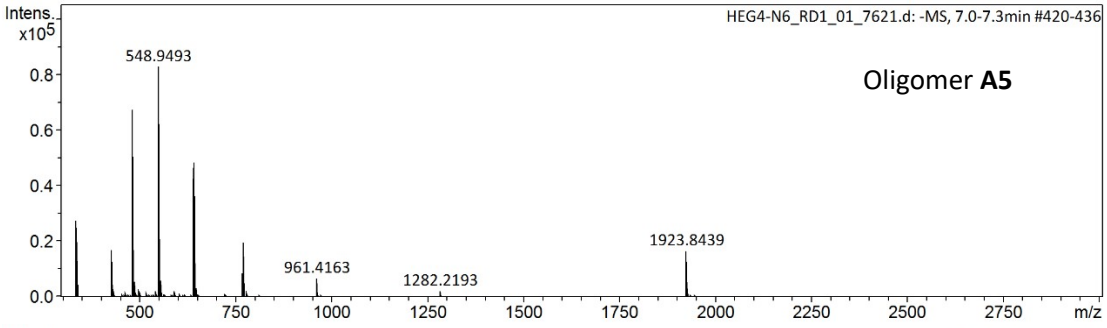
HEG4-N6_RD1_01_7621.d: -MS, 7.0-7.3min #420-436
Intens.
x10^5
548.9493
961.4163
1282.2193
1923.8439
m/z
Oligomer **A5**

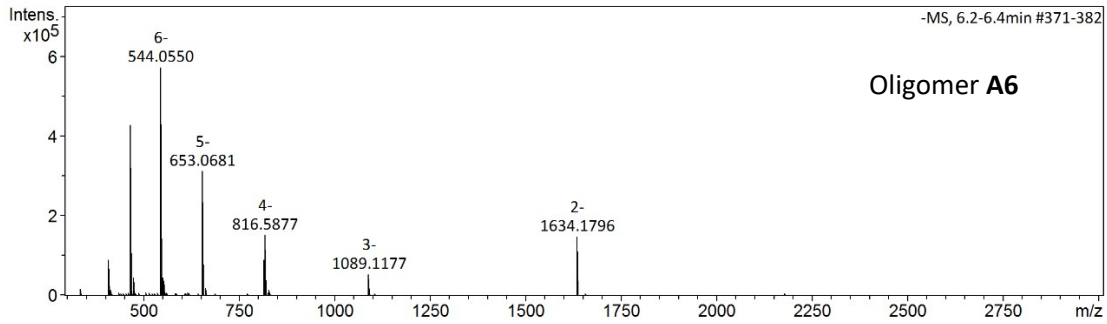
-MS, 6.2-6.4min #371-382
Intens.
x10^5
6-
544.0550
5-
653.0681
4-
816.5877
3-
1089.1177
2-
1634.1796
m/z
Oligomer **A6**

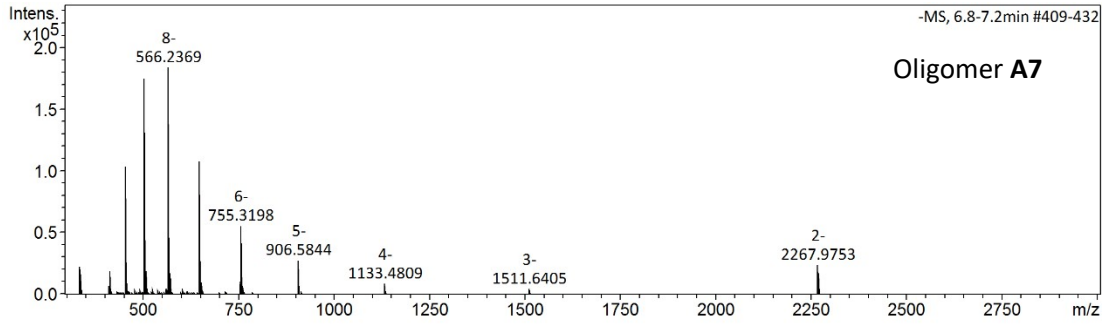
-MS, 6.8-7.2min #409-432
Intens.
x10^5
8-
566.2369
6-
755.3198
5-
906.5844
4-
1133.4809
3-
1511.6405
2-
2267.9753
m/z
Oligomer **A7**

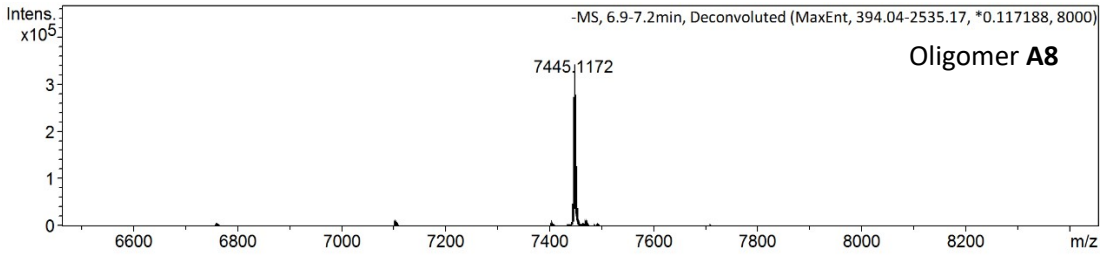
-MS, 6.9-7.2min, Deconvoluted (MaxEnt, 394.04-2535.17, *0.117188, 8000)
Intens.
x10^5
7445.1172
m/z
Oligomer **A8**

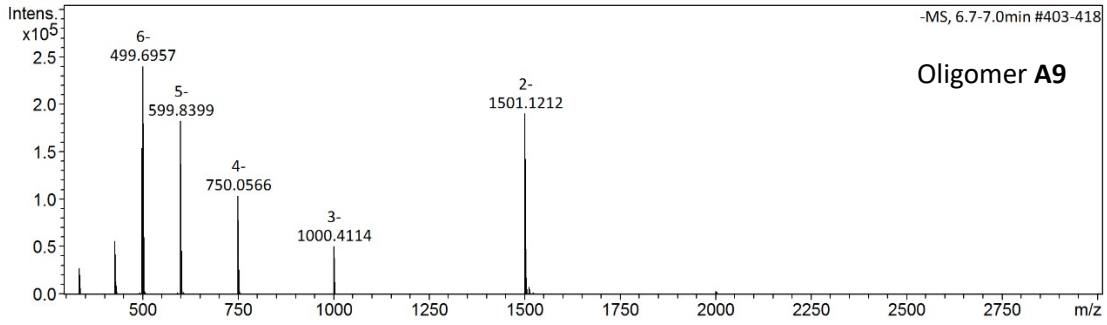
-MS, 6.7-7.0min #403-418
Intens.
x10^5
6-
499.6957
5-
599.8399
4-
750.0566
3-
1000.4114
2-
1501.1212
m/z
Oligomer **A9**

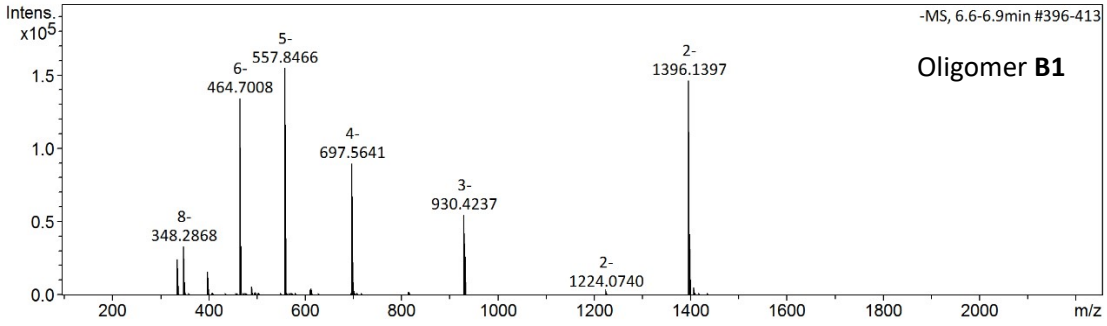
Intens.
x10^5
-MS, 6.6-6.9min #396-413
Oligomer B1
5-
557.8466
6-
464.7008
2-
1396.1397
4-
697.5641
3-
930.4237
8-
348.2868
2-
1224.0740
m/z

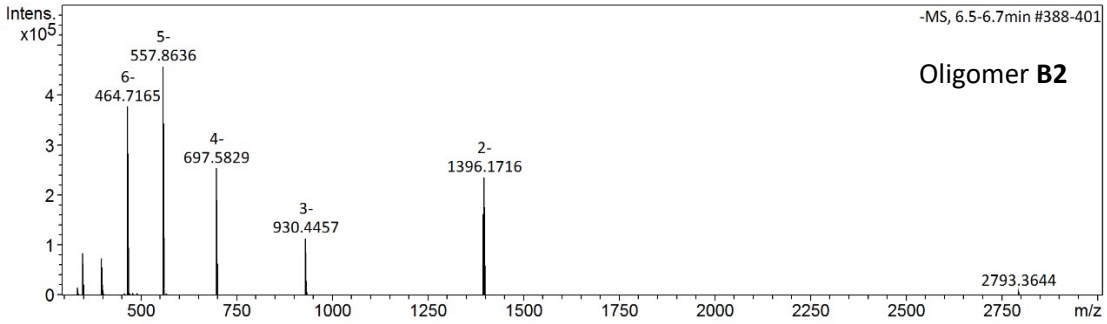
Intens.
x10^5
-MS, 6.5-6.7min #388-401
Oligomer B2
5-
557.8636
6-
464.7165
4-
697.5829
2-
1396.1716
3-
930.4457
2793.3644
m/z

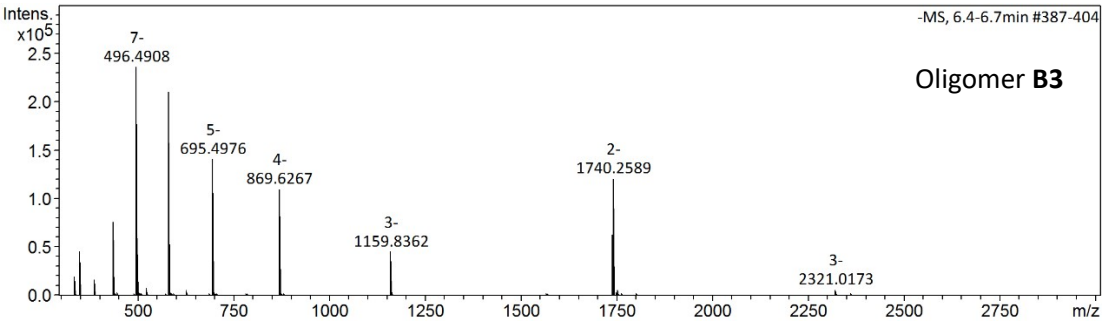
Intens.
x10^5
-MS, 6.4-6.7min #387-404
Oligomer B3
7-
496.4908
5-
695.4976
4-
869.6267
2-
1740.2589
3-
1159.8362
3-
2321.0173
m/z

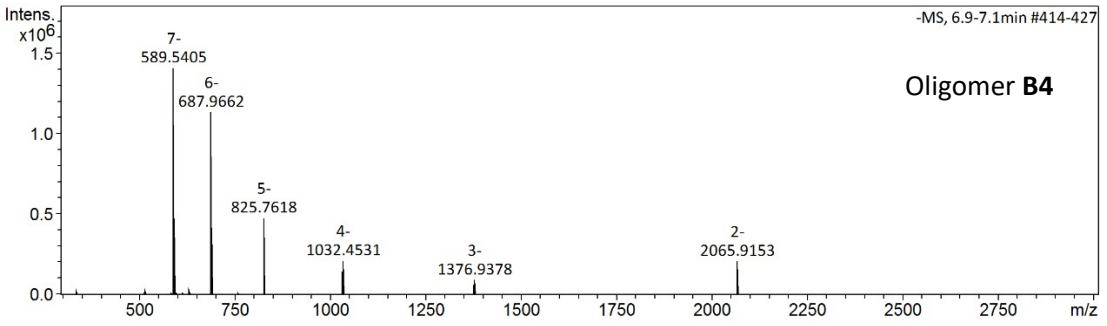
Intens.
x10^6
-MS, 6.9-7.1min #414-427
Oligomer B4
7-
589.5405
6-
687.9662
5-
825.7618
4-
1032.4531
3-
1376.9378
2-
2065.9153
m/z

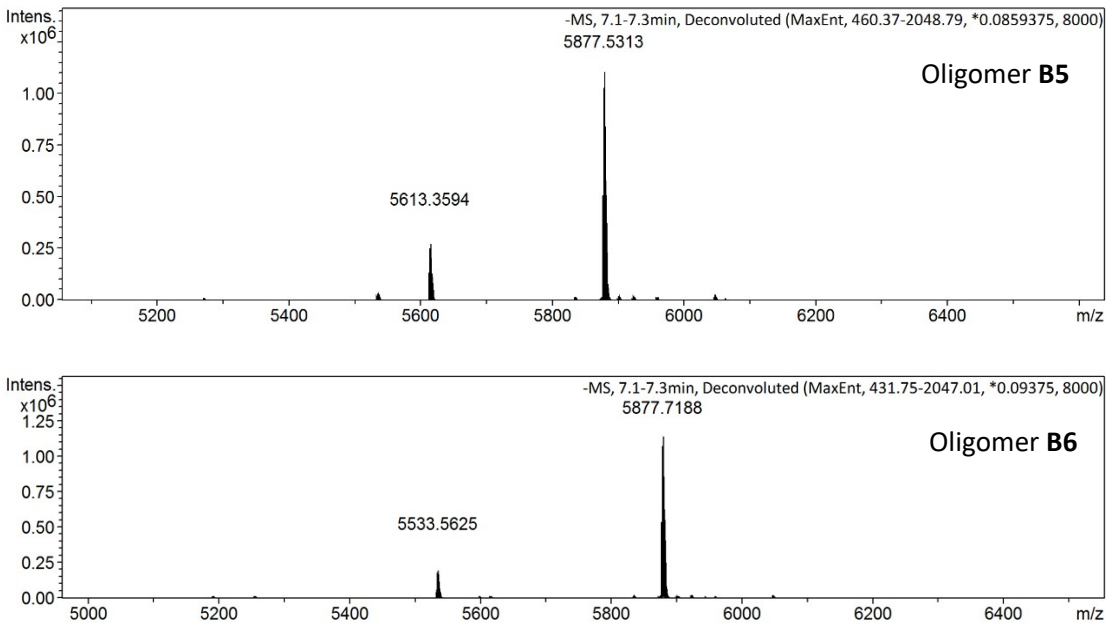

Figure S2. MS data for sequence-controlled oligomers, negative mode. Almost all peaks can be associated with a (M-x)/x anion. For oligomers **A8**, **B5**, **B6,** the data was processed and deconvoluted using the Bruker DataAnalysis software version 4.1. Masses reported are exact masses.

7. Atomic Force Microscopy

7.1. Dry conditions

We tried to visualize the structures shown using different buffers (namely TAMg, TBS and PBS) at concentrations close to the concentrations we usually work with in the case of DNA nanostructures, 1 µM to 10 µM. We were initially washing the mica with MilliQ water after sample deposition to clean the surface from salts that would get stuck on the surface. However, all our attempts with these conditions led to non-reproducible results.

We therefore decided to change 3 crucial parameters: nanostructure concentration, ionic strength of the buffer and avoided washing steps. This last option is usually not recommended when working with buffers. Salts can sometimes form aggregates that may be confused with the structures one expects to see. To allow the use of unwashed samples, we decided to image a negative control without oligomer at the beginning of each AFM session. We never observed patterns similar to the ones described in this article.

Spherical micelles samples were tried using the same conditions than **A4** and **A7.** Only **A8** and **B2** led to reproducible results in dry conditions.

Unless otherwise noticed, samples were annealed in TA5Mg from 95 °C to 4 °C at 250 µM during 1 h. Right after, samples were diluted to the desired concentration. 4 µL of this solution was deposited on a freshly cleaved mica surface (ca. 7 x 7 mm) and allowed to adsorb for 2-3 min. Samples were not washed and were dried under a flow of argon followed by vacuum for 3-4 h prior to imaging. Cantilevers used were Scan-Asyst Fluid +. Images were captured at scan rates between 0.5 and 1.5 Hz at a resolution of 512 x 512 pixels or 256 x 256 pixels for a few images. The gain was set at 20. The peak force setpoint, z-limit and peak force amplitude were set automatically by the software. Images were processed using Nanoscope Analysis 1.5 software (Bruker).

At high concentration (100 µM), in TAMg instead of TA5Mg, nanosheets could be observed in rare occasions.

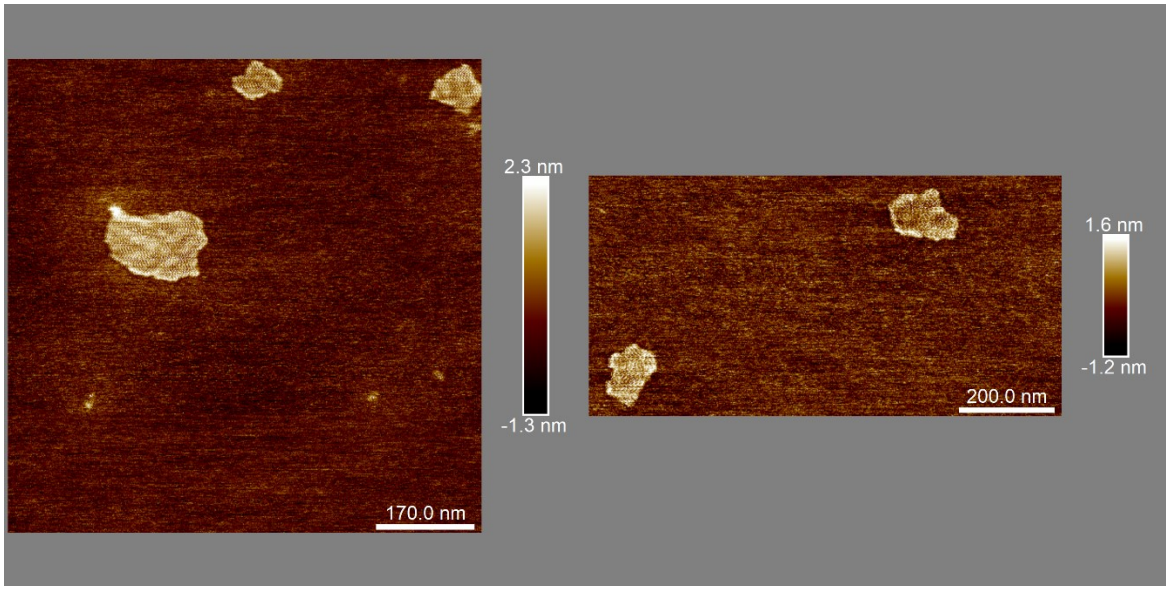

Figure S3. Oligomer **A4**, 100 µM, TAMg,

When adding $NiCl_2$ after annealing and dilution to reach 1 μM, the optical camera showed an irregular surface, probably due to the irregular salt deposition.

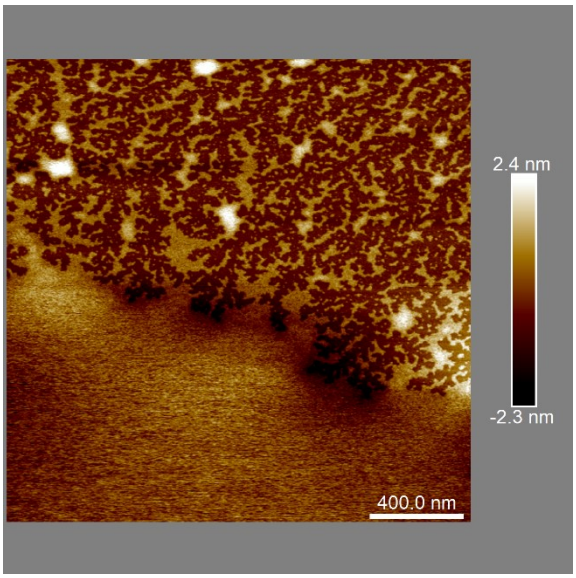

Figure S4. Negative control, 1 μM $NiCl_2$. We believe there is a layer of nickel and magnesium salts formed on half the image at the bottom.

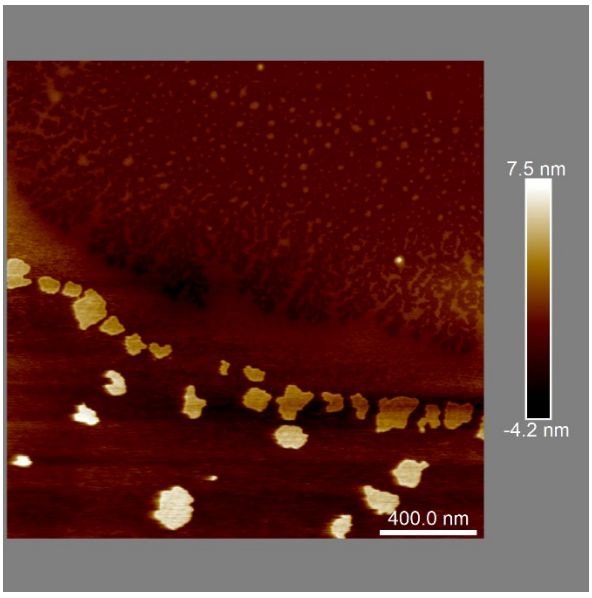

Figure S5. Oligomer **A4**, 10 μM, 1 μM $NiCl_2$. We believe the patches of nanosheets bind to the layer of nickel and magnesium salts.

Once we focus on the areas with the salts layer and increase the oligomer concentration, we started to get good images of the nanosheets.

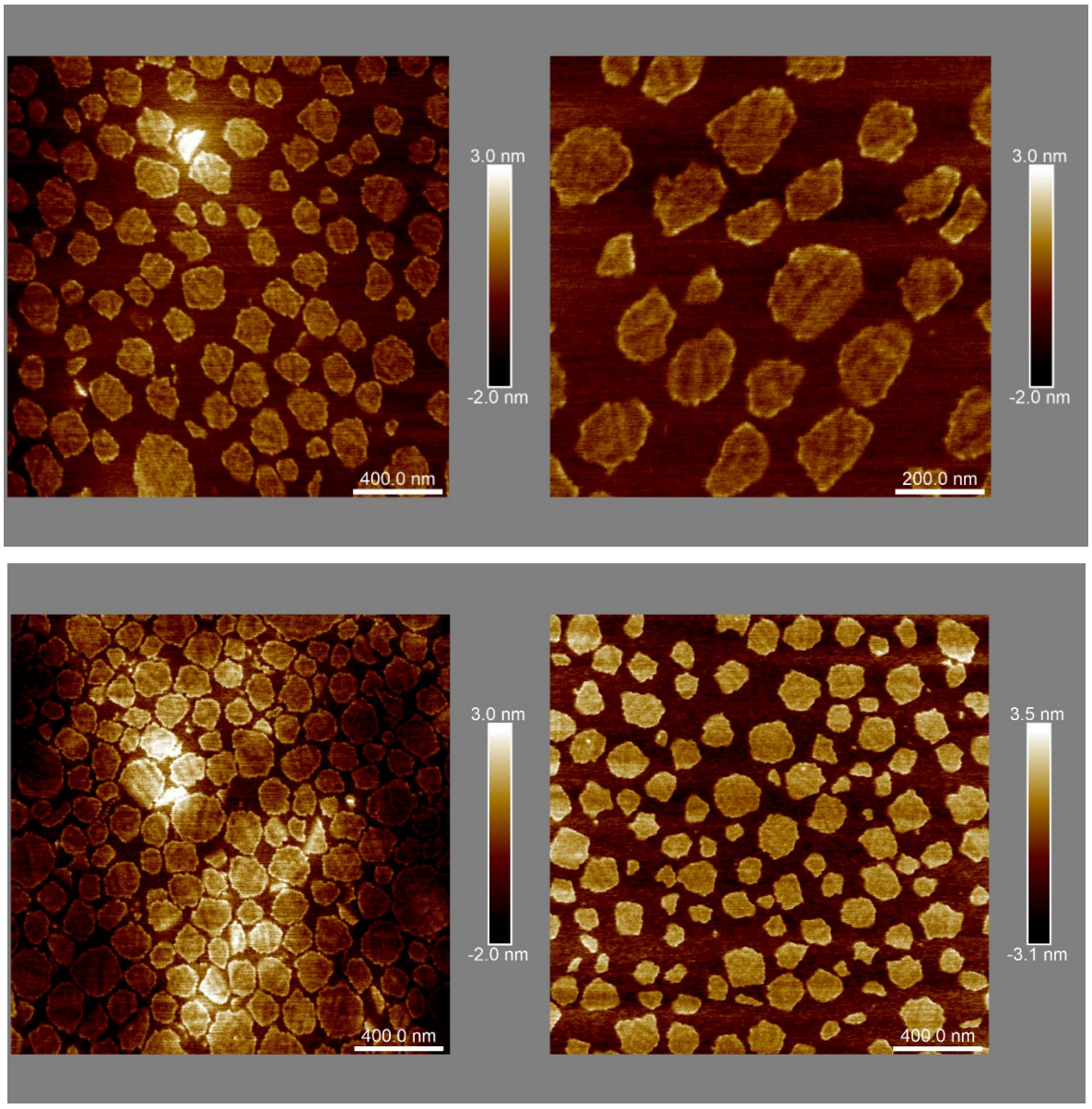

Figure S6. Oligomer **A4**, 50 µM 1 µM $NiCl_2$.

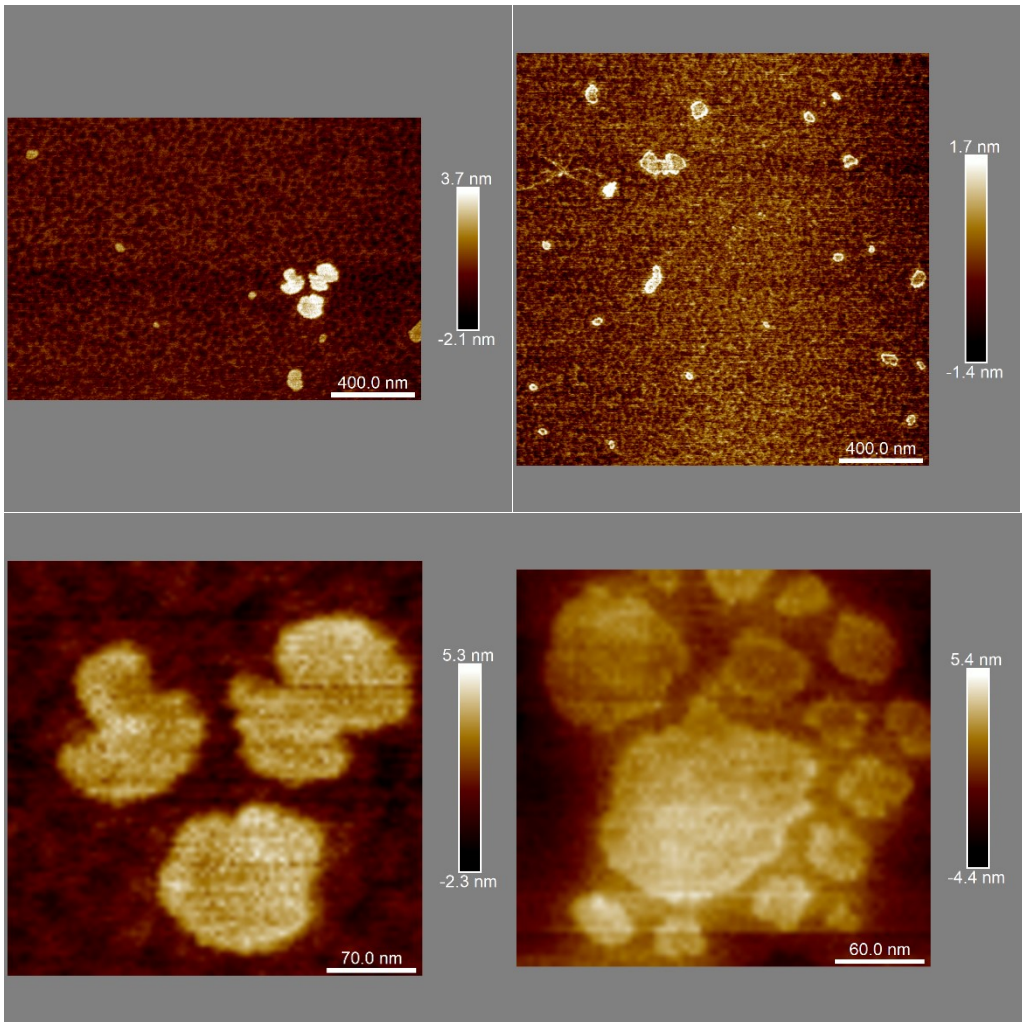

Figure S7. Oligomer **A7**, 50 µM 1 µM $NiCl_2$.

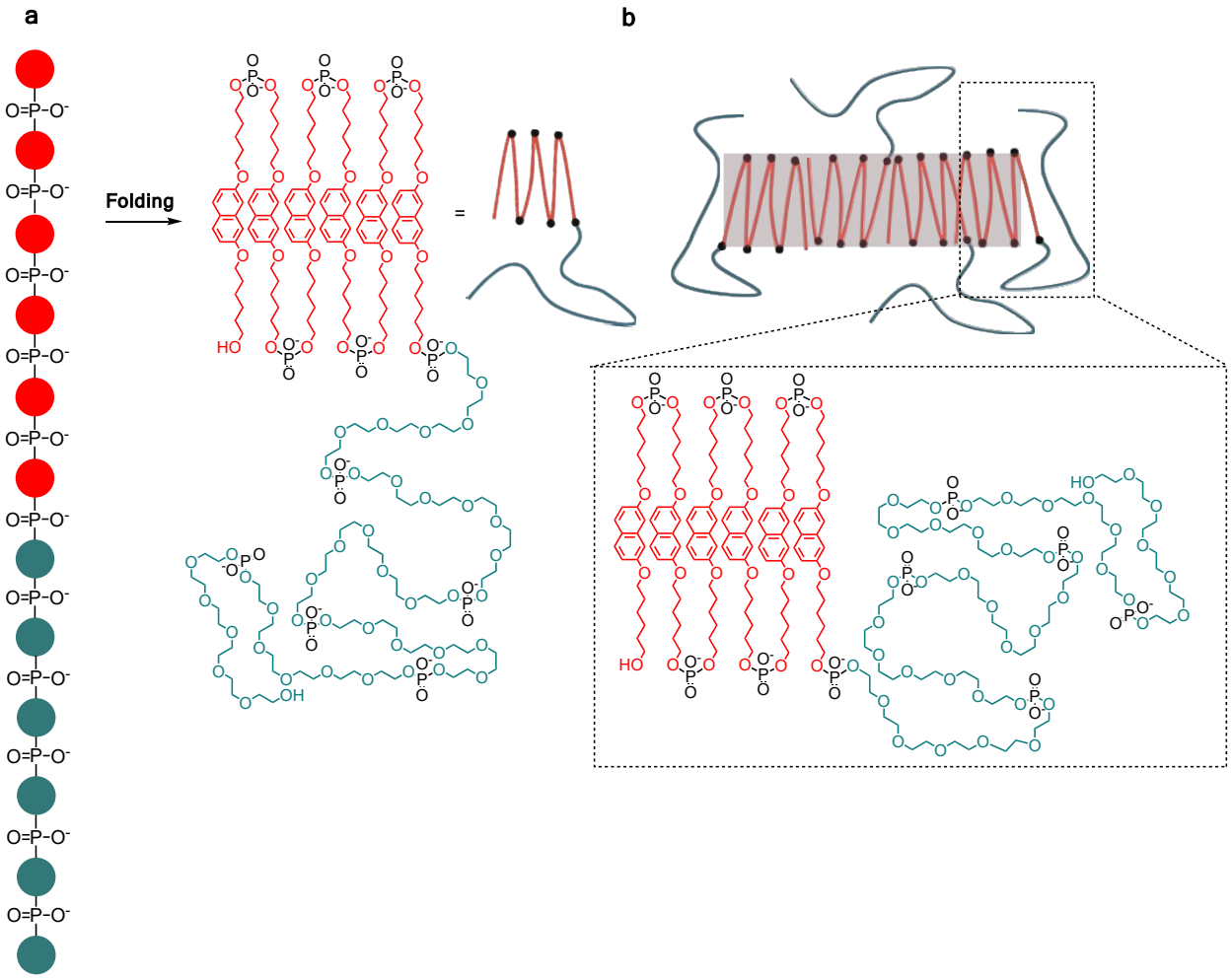

Figure S8. (a) Folding of the **A7** (HEG_6-NAP_6) monomer into a zig-zag conformation to induce (b) the formation of nanosheets with **HEG** chains terminating the side growth. As compared to Figure 4, the longer **HEG** chains with six monomers instead of four leads to more efficient capping of the hydrophobic sides, resulting in fewer monomers being incorporated per nanosheet and smaller sheet overall.

Imaging of these structures was also tried on HOPG. However, with or without washing steps and without nickel chloride, negative controls and samples were found to be too similar to be appropriately analyzed.

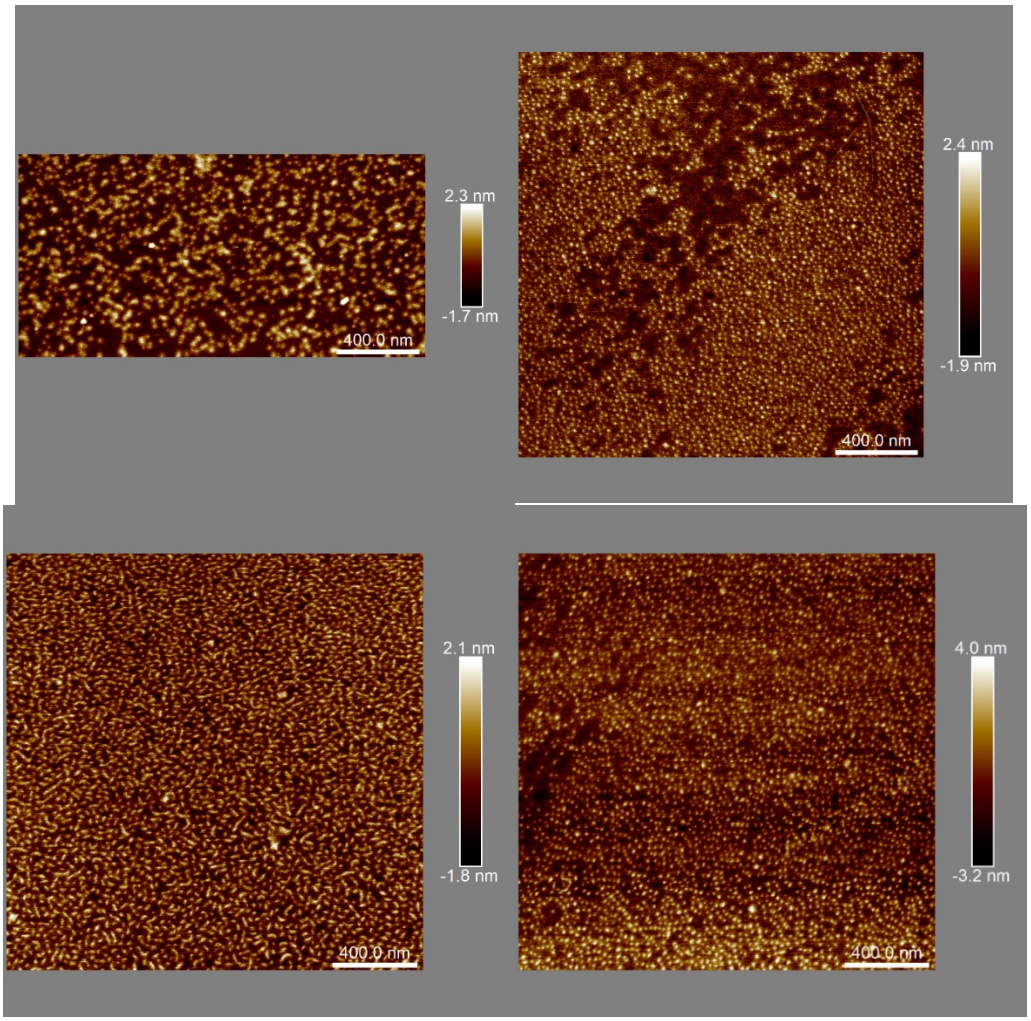

Figure S9. Oligomer **A3** (top left), 50 µM and oligomer **A8** (all other images), 10 µM. For these oligomers, mica was pretreated with a 20 mM $NiCl_2$ solution instead of adding $NiCl_2$ in the sample before deposition.

For **A8** (**HEG_{12}-NAP_8**), hydrodynamic diameter is larger than expected from the AFM images. We believe interaction between mica, Ni^{2+} ions and **A8** had an impact on its self-assembly.

7.2. Fluid conditions

Prior to imaging, mica was treated with a 5 mM $NiCl_2$ solution: 100 µL were deposited on the freshly cleaved mica surface (ca. 12 x 12 mm) and left for 5 min. The solution was then dried using a nitrogen flow. To ensure that Ni^{2+} does not perturb the self-assembly of these structures, it was first deposited on mica prior to the deposition of the structures.

Unless otherwise noticed, samples were annealed in TA5Mg from 95 °C to 4 °C at 250 µM during 1 h. Right after, samples were diluted to the desired concentration. 5 µL of this solution was deposited on the pretreated mica surface, allowed to adsorb for 2-3 min and 70 µL of TA5Mg was added. Excess was immediately removed using filter paper and dried under a nitrogen flow. After placing the sample on the AFM sample stage, fluid cell was positioned on the sample (MTFML fluid cell, Bruker) and 40 µL of 1x TA5Mg was injected into the cell.
Cantilevers used were Scan-Asyst Fluid +. Images were captured at scan rates between 0.5 and 1.5 Hz at a resolution of 512 x 512 pixels or 256 x 256 pixels for a few images. The gain was set at 20 and the z-limit at 1 µm. The peak force setpoint and peak force amplitude were set automatically by the software. Images were processed using Nanoscope Analysis 1.5 software (Bruker).

The good correlation between what is observed on AFM using this method and the data obtained by DLS and AGE make us confident that no significant morphological change takes place upon deposition on Ni^{2+}-coated mica.

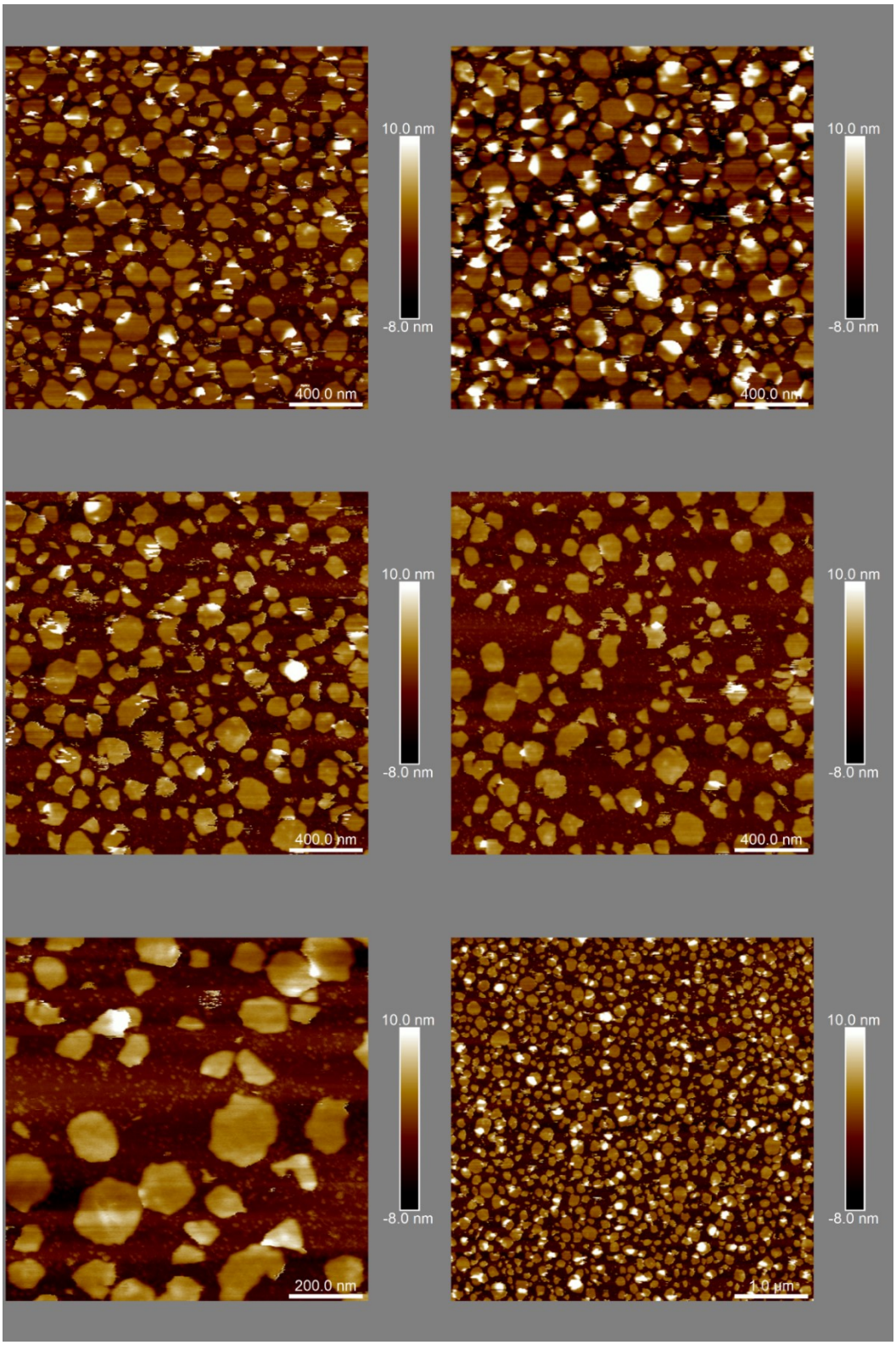

Figure S10. Oligomer **A4**, 50 µM.

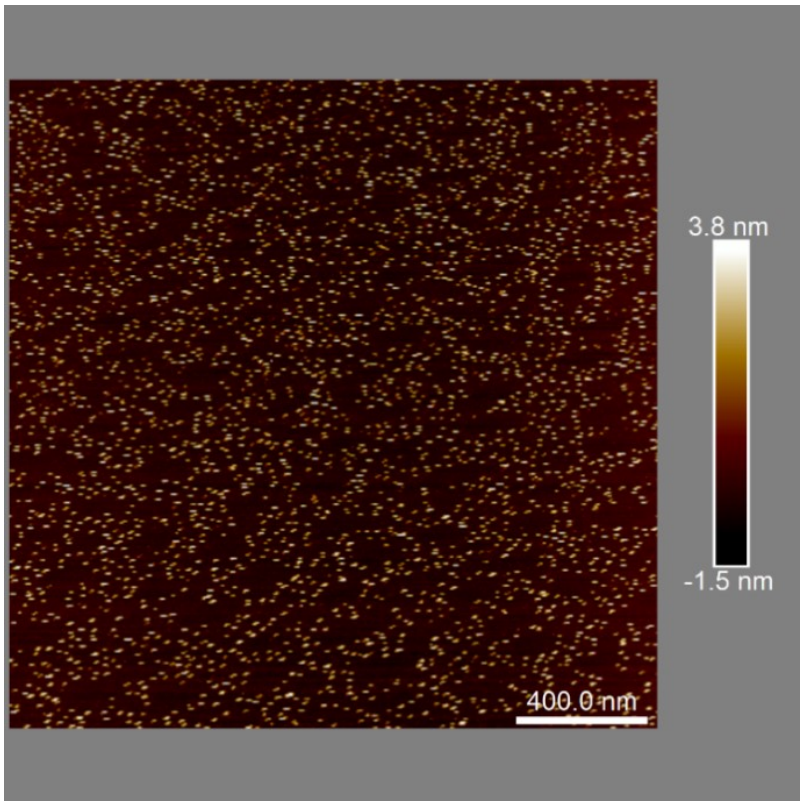

Figure S11. Oligomer **A8,** 10 μM.

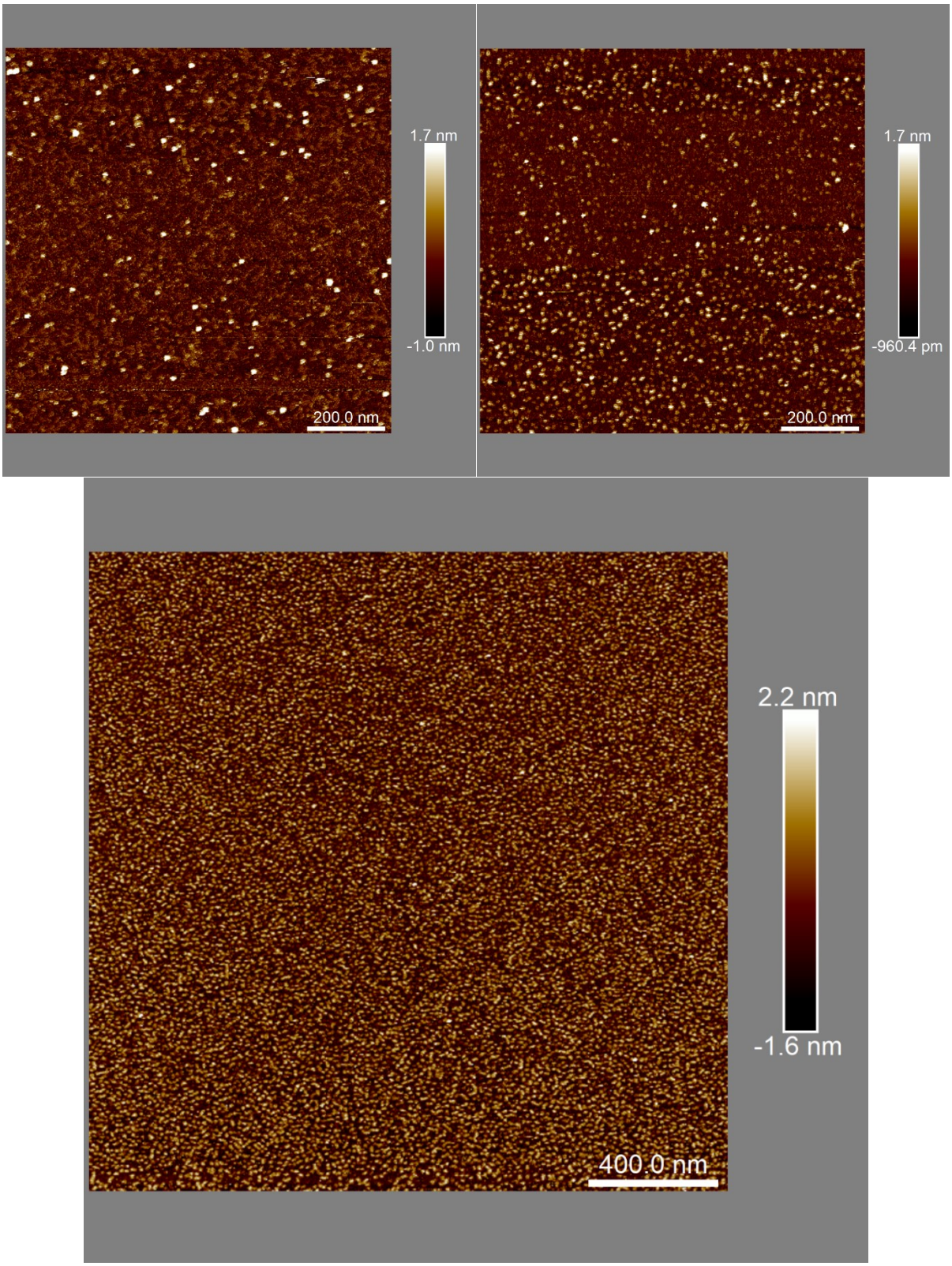

Figure S12. Oligomer **B2**, 1 μM (top) and 10 μM (bottom).

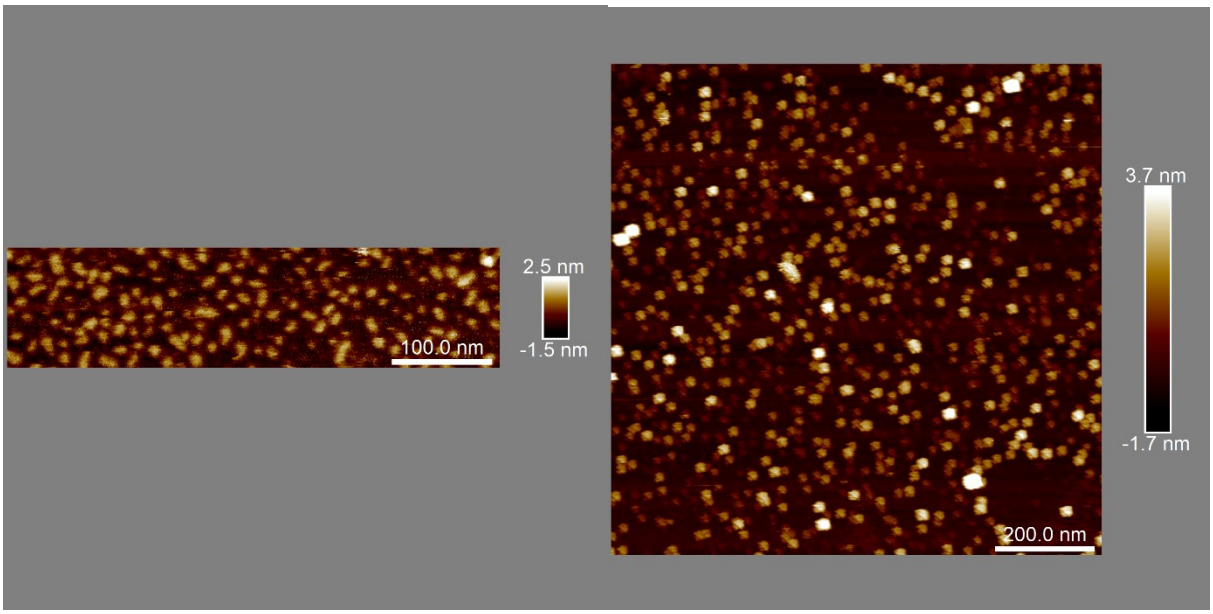

Figure S13. Oligomer **B3**, 50 μM.

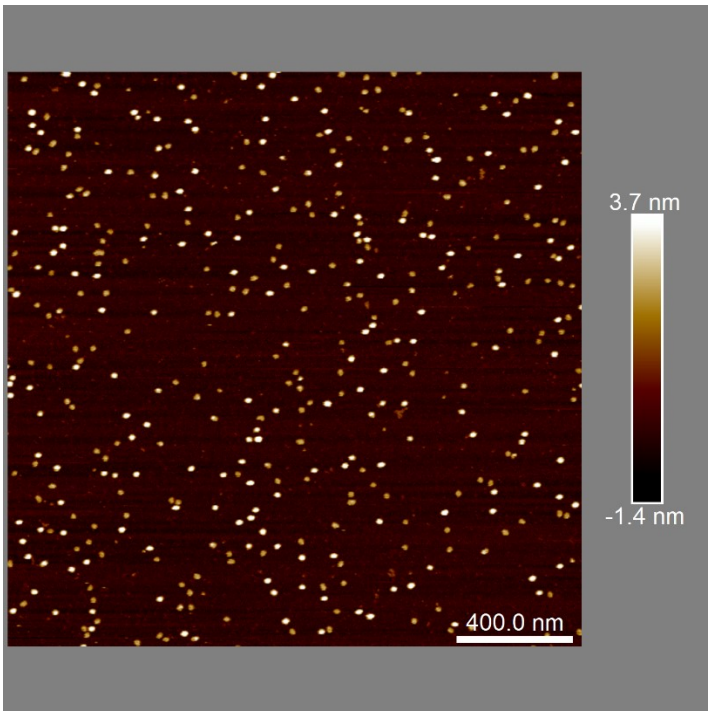

Figure S14. Oligomer **B5**, 1 μM.

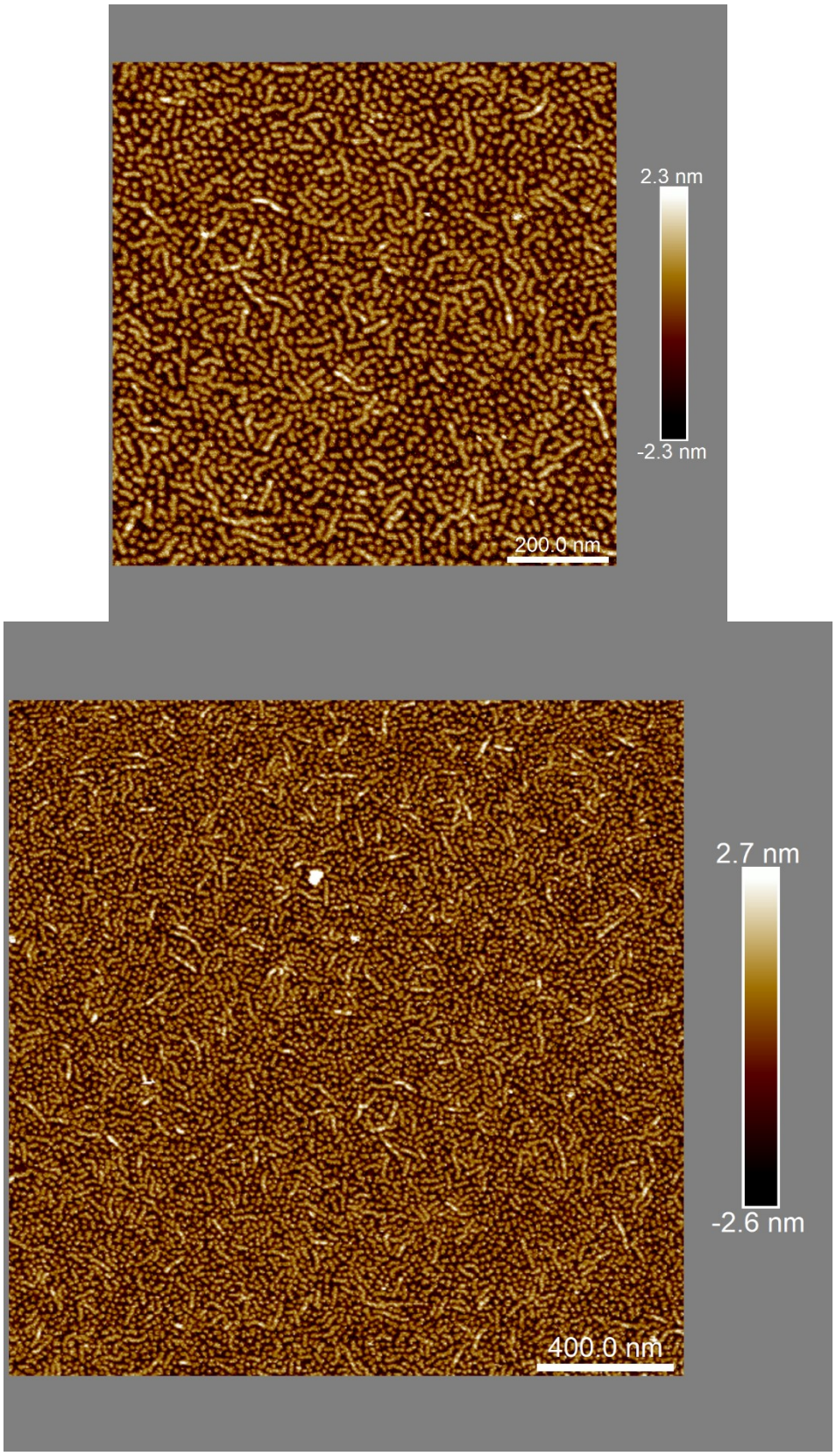

Figure S15. Oligomer **B6**, 10 μM.

8. Transmission Electron Microscopy

First trials were done using a high-voltage TEM but structures revealed to be hard to image, noticeably due to the fact that the **HEG** moieties are known to "burn" under a high energy electron beam. For TEM, the high amount of salts was less problematic because most samples were washed with water before imaging. However, we still took images of negative controls (without nanostructure) to make sure of the presence of the nanosheets.

Unless otherwise noticed, samples were annealed in TA5Mg from 95 °C to 4 °C at 250 μM during 1 h. Right after, samples were diluted to the desired concentration (usually 25 μM). 4 μL of this solution was deposited on a TEM carbon film coated copper EM grid (300 mesh Cu grid with holey/dbl carbon films, from Pacific Grid Tech), allowed to adsorb for 2-3 min and washed twice with MilliQ wster to remove salt excess. The grids were then kept under vacuum for at least 3 h.

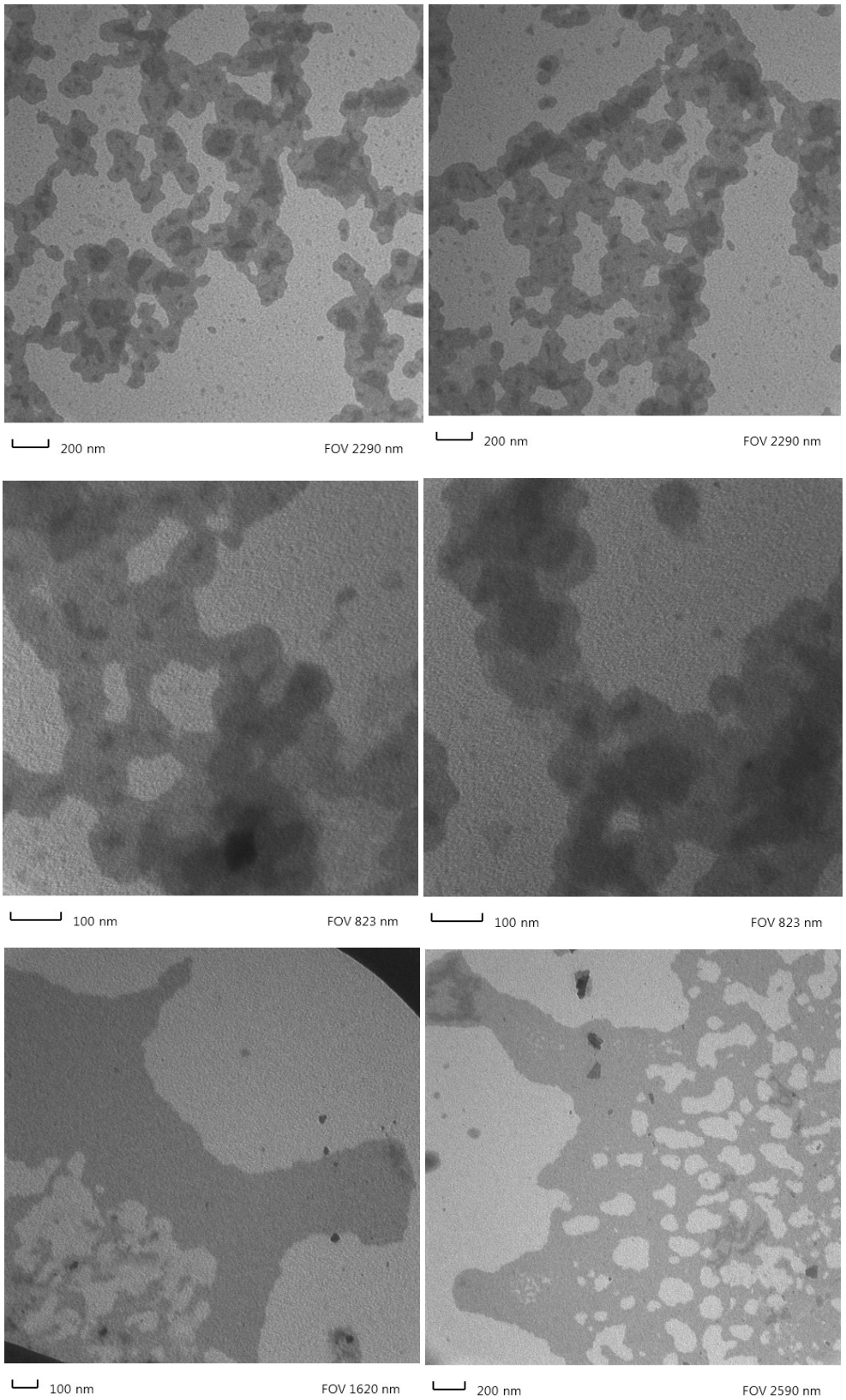

Figure S16. Oligomer **A4**, 25 μM. No wash had been performed for the two bottom images.

9. Dynamic Light Scattering

Dynamics V6 was used for data collection and analysis. A cumulants fit model was used to confirm/infirm the presence and determine the diffusion coefficients of a monomodal population of micellar aggregates. Hydrodynamic diameters reported in the main text were calculated with Dynamics V6 globular protein model. Sterile water and TA5Mg were filtered using a 0.2 µm nylon syringe filter before use for DLS sample preparation. All measurements were carried out at 20 °C after annealing of the constructs in TA5Mg from 95 °C to 4 °C at 250 µM during 1 h. Concentration of the sample is lowered to 25 µM after annealing. All the measurements were done at least in duplicates.

Table S2. DLS characterization of selected sequence-defined oligo(phosphodiester)s.

Oligomer	Sequence	Diffusion coefficient [10^{-7} $cm^2.s^{-1}$]
A3	**HEG_4-NAP_3**	3.0
A4	**HEG_4-NAP_4**	0.44
A6	**HEG_6-NAP_3**	3.1
A7	**HEG_6-NAP_6**	0.96
A8	**NAP_8-HEG_{12}**	1.1
B3	**HEG_6-NAP-$C12_4$**	3.6
B5	**HEG_6-NAP-PFC_4-$C12_4$**	2.8
B6	**HEG_6-NAP-$C12_4$-PFC_4**	2.2

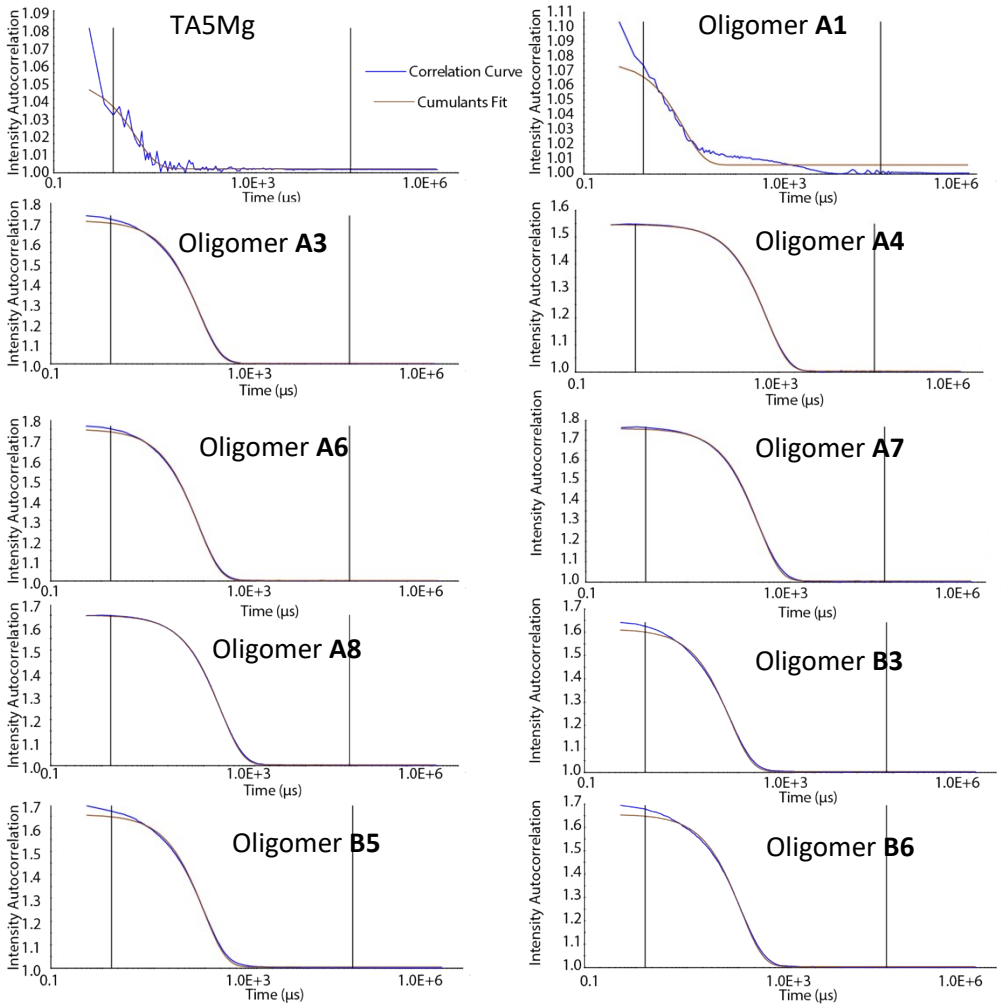

Figure S17. Dynamic light scattering on oligomers. Representative DLS intensity correlation functions for 25 µM solutions. Control sample and oligomer **A1** show poor fit because the particles are too small to be accurately analyzed. In contrast the data for self-assembling oligomers reveals excellent correlation even for oligomer **A4** and **A7** which does not assemble into spherical objects when deposited on a substrate.

Due to its perfluorocarbon core, we believe **B5** and **B6** could self-assemble without requiring the magnesium cations presence. However, DLS measurements seem to indicate that no self-assembly occurs after annealing in Milli-Q water. Buffering the same solution with a magnesium containing solution triggered instantaneous self-assembly of **B6**. Oligomers **B5** and **B6** were annealed with the same protocol in MilliQ water and analyzed similarly.

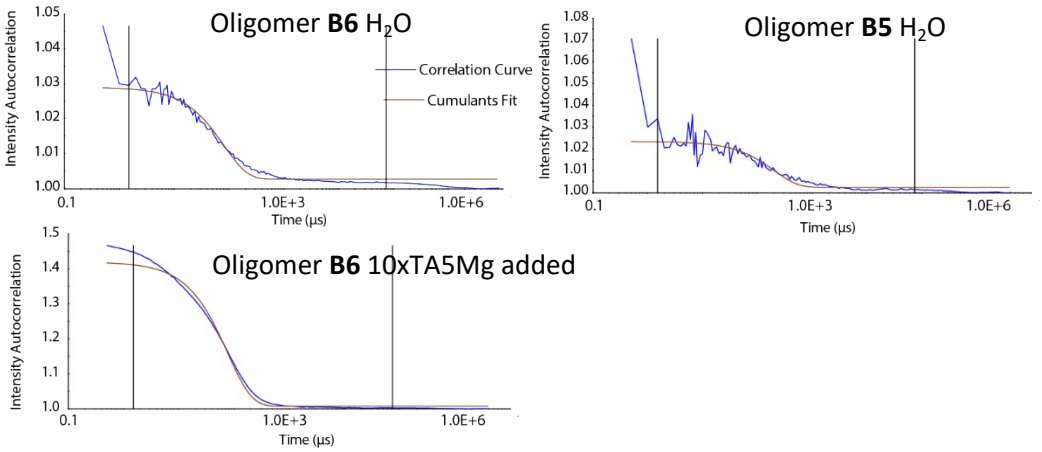

Figure S18. Dynamic light scattering on oligomers **B5** and **B6** in water after annealing and once 10xTA5Mg has been added to obtain 1xTA5Mg. Representative DLS intensity correlation functions for 25 µM solutions. In water, it looks like **B5** and **B6** are not self-assembling whereas addition of buffer triggers self-assembly. Fit is not as good as on Figure S3, probably because the sample has not been annealed in TA5Mg here.

10. Gel Electrophoresis Analysis

20% denaturing Polyacrylamide Gel Electrophoresis (PAGE) was carried out at room temperature for 30 min at 250 V followed by 1 h at 500 V. 1x TBE buffer was used and the concentration of urea in the gel was 7 M. For each lane 5 µL of sample in water was added to 5 µL of 8 M urea. Amount of the oligomer to load was done according to the principle that the more **NAP** the oligo contains, the more it will have affinity for GelRed™. Therefore, respectively 0.8, 0.6, 0.4, 0.3, 0.6 and 0.3 nmol of **A2**, **A3**, **A4, A5**, **A6** and **A7** were loaded. The oligomers were visualized by incubation with GelRed™ for 10 min.

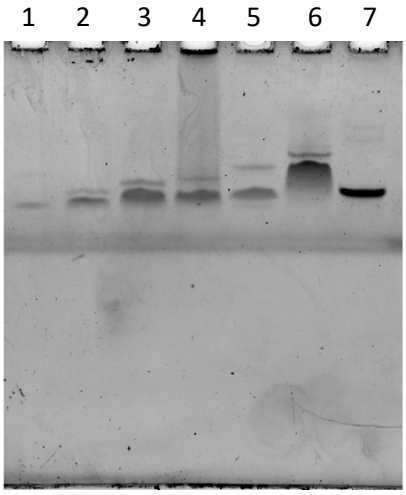

Figure S19. Denaturing gel (PAGE 20%) with oligomers **A2, A3, A4, A5, A6, A7** followed by a DNA 22mer in respectively lanes 1 to 7.

2.5% agarose gel electrophoresis (AGE) was carried out in TAMg at 4 °C for 2 h at 80 V. Gel was cast in TAMg and the samples were already annealed with the same method detailed in section 7. Respectively 1.1, 0.9, 0.7, 0.5, 0.3, 0.6, 0.3 and 0.6 nmol of **A1**, **A2**, **A3**, **A4, A5**, **A6, A7** and **A9** in 10 µl of TA5Mg. 2 nmol of **B** oligomers were loaded. 2 µl of glycerol were added to the samples before loading. The bands for all gels were visualized by incubation with GelRed™. We believe self-assembled nanostructures are more likely to recruit GelRed® molecules than free oligomers leading to better sensitivity.

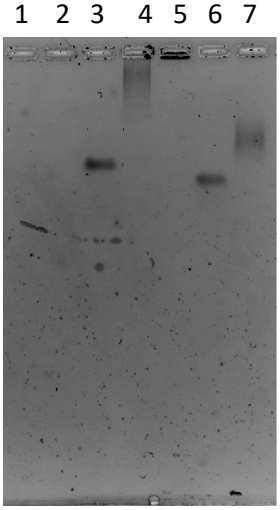

Figure S20. Full agarose gel (AGE 2.5%) with oligomers **A1, A2, A3, A4, A5, A6, A7** in respectively lanes 1 to 7.

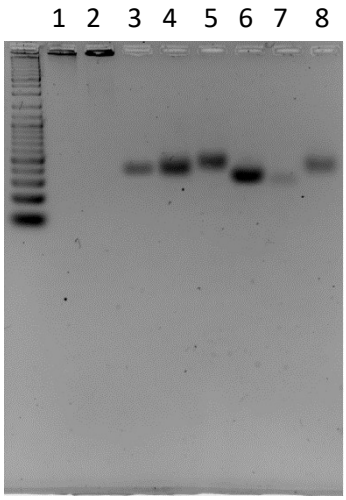

Figure S21. Full agarose gel (AGE 2.5%) with oligomers **A5, A9, B2, B6, B5, B3, B1, B4** in respectively lanes 1 to 8. The DNA ladder used is the O'Gene Ruler Mix from ThermoScientific.

11. Supporting References

[1] D. de Rochambeau, Y. Sun, M. Barlog, H. S. Bazzi, H. F. Sleiman, *J. Org. Chem.* **2018**, *83* , 9774–9786.

[2] D de Rochambeau, M. Barłóg, T. G. W. Edwardson, J. J. Fakhoury, R. S. Stein, H S. Bazzib, H. F. Sleiman, *Polym. Chem.* **2016**, *7*, 4998–5003.